Characterization and optimization of a ring self-pumped phase conjugate mirror at 1.06 Mm with BaTiO3:Rh

Nicolas Huot, Jean-Michel Jonathan, Gérald Roosen, Daniel Rytz

Characterization and optimization of a ring self-pumped phase-conjugate mirror at 1.06 μm with $BaTiO_3$:Rh

N. Huot, J. M. C. Jonathan, and G. Roosen

Institut d'Optique Théorique et Appliquée, Unité de Recherche Associée 14 au Centre National de la Recherche Scientifique, Bâtiment 503, B.P. 147, 91403 Orsay Cedex, France

D. Rytz

Forschungsinstitut für mineralische und metallische Werkstoffe, Edelsteine/Edelmetalle GmbH, Struthstrasse, 2, 55743 Idar-Oberstein, Germany

Received September 2, 1997; revised manuscript received November 21, 1997

We optimize the ring self-pumped phase-conjugate mirror at 1.06 μm. With cw as well as nanosecond illumination the photorefractive efficiency is higher than 90%. Therefore the reflectivity (79%) is limited only by the transmission of the loop. Another relevant characteristic is the time needed to increase the reflectivity from 10% to 90% of its maximum value, which is as little as 12 s at 5 W cm^{-2} in the cw regime. In the nanosecond regime, 90 J cm^{-2} is needed. We study the response to an abrupt change in the incident wave front, taking into account the three-prism system inserted in the loop. © 1998 Optical Society of America [S0740-3224(98)00707-3]

OCIS codes: 190.5330, 190.5040.

1. INTRODUCTION

Rhodium-doped barium titanate ($BaTiO_3$:Rh) is interesting because of its significant response at laser diode (780–860-nm) and Nd:YAG (1.06-μm) wavelengths. Beam cleanup in the visible range, previously described,[1] was recently demonstrated with laser diodes at 860 nm with $BaTiO_3$:Rh.[2] Laser diode coupling has also been achieved at 820 nm with an undoped $BaTiO_3$ crystal.[3] In self-pumped phase conjugation, undoped $BaTiO_3$ had been shown to present some response at 1.09 μm, although the response time is poor and the reflectivity is limited to 18%.[4] As the result of rhodium doping, $BaTiO_3$:Rh has shown significant phase-conjugate reflectivities up to a wavelength of 0.99 μm in a total internal reflection geometry.[5] More recently, a reflectivity of 55% was measured at 1.06 μm in a $BaTiO_3$:Rh crystal in the internal loop geometry in the cw illumination regime.[6]

We measured a high photorefractive two-wave mixing gain at 1.06 μm as well in the cw illumination regime (23 cm^{-1}),[7] and in the nanosecond illumination regime (16.6 cm^{-1}) (Ref. 8) in $BaTiO_3$:Rh. Moreover, at 1.06 μm for nanosecond pulsed illumination up to 20 MW cm^{-2} this crystal exhibits no intensity-dependent electron–hole competition and no saturation of the density of free carriers (holes).[8] Both these effects are observed in the visible range: The photorefractive gain is affected by an intensity-dependent electron–hole competition leading to an inversion of the sign of the photorefractive gain, while the time constant of the photorefractive effect saturates for high illuminations.[9,10] We also observed that similar fluences are required for recording a grating in the cw and nanosecond illumination regimes ($\sim$100 J cm^{-2} in the counterpropagating geometry). This observation encouraged us to perform self-pumped phase conjugation at 1.06 μm with $BaTiO_3$:Rh crystals. After an optimization of the geometry of the crystal to get rid of parasitic spurious beams, we experimented with ring self-pumped phase conjugation and demonstrated reflectivities as high as 50% in the cw illumination regime without any particular grating spacing optimization.[11]

In this paper we study the reproducibility of the photorefractive $BaTiO_3$: Rh crystals, which is important for practical applications. We present an optimization of the performance of the ring self-pumped phase-conjugate mirror at 1.06 μm. In the nanosecond illumination regime we select the phase-conjugate beam by using a three-prism system and demonstrate efficient phase conjugation. Then we use this optimized nonlinear mirror to study the influence of an abrupt change in the wave front of the incident beam.

2. REPRODUCIBILITY OF THE $BaTiO_3$:Rh CRYSTALS

Applications rely on the reproducibility of performance of the photorefractive crystals, which may present significant variations even when the crystals are cut from the same boule. We assessed this reproducibility in the case of $BaTiO_3$:Rh, using two crystals from the same boule, to which we refer as X16-5/2 [a 0°-cut 5.8 mm $\times$ 4.5 mm $\times$ 8.5($=c$)mm sample] and X16-45 (a 45°-cut 3.5-mm-thick crystal). The boule was grown with 1000 parts in 10^6 of rhodium in the melt. At 1.06 μm in the cw illumination regime the steady-state light-induced absorption

0740-3224/98/071992-08$15.00

$\Delta\alpha$ and its initial slope $[(\partial\Delta\alpha)/(\partial t)]_{t=0}$ at $I = 1.1$ W cm^{-2}, as well as the effective density of traps N_{eff} at saturation in intensity, are relevant parameters.[12] Γ, the two-wave mixing exponential gain at saturation in intensity, is directly related to N_{eff} and to the geometry of the experiment. Therefore, instead of N_{eff}, we compared Γ for different samples in the same recording configuration. To measure Γ by two-wave mixing we used an ordinary polarization to ensure a low gain, and the counterpropagating geometry where the time constant is the shortest. We estimated the time constant τ_{ph} for the rise of the space-charge field in the counterpropagating geometry for a given intensity from the rise time of Γ, using a simplified model valid for small gains.[8] Moreover, we estimated the erasure time in the dark τ_{dark} and verified that the ratio $\tau_{\text{dark}}/\tau_{\text{ph}}$ remained much larger than unity. We also measured the absorption of the material at saturation of the light-induced absorption. All these values, given in Table 1, show that the properties of these two crystals are quite similar and indicate a reasonable homogeneity of the boule. For sample X16-45, τ_{ph} and Γ are given for $\beta = 45°$ (β is the angle between the grating wave vector and the c axis), and therefore they cannot be directly compared with those obtained at $\beta = 0°$ for other crystals.

A second series of characterizations was performed in the same conditions, with two crystals X17-6/3 [6.6 mm $\times$ 5.0 mm $\times$ 5.2(=c)mm] and X17-6/4 [7.0 mm $\times$ 5.1 mm $\times$ 6.2(=c)mm] both cut at 0° from another boule, also grown with 1000 parts in 10^6 of rhodium in the melt in the same conditions as for the previous series, in an attempt to reproduce the properties of the X16 crystals. Observe from Table 1 that the data for the two crystals from the new boule are quite similar, except for the value of τ_{dark}. Nevertheless, the high value of the ratio $\tau_{\text{dark}}/\tau_{\text{ph}}$ ensures that the photorefractive gain is well saturated for all the samples in these experimental conditions. The results obtained for the two boules are very close, indicating that the control of the crystal growth and doping now permits the production of reasonably reproducible $BaTiO_3$:Rh crystals for applications at 1.06 μm, where the dark decay is not an important parameter.

3. OPTIMIZATION OF THE PERFORMANCES OF THE RING SELF-PUMPED PHASE-CONJUGATE MIRROR

In all the experiments described below we used the X16-45 sample. For dynamic wave-front correction of 10-ns pulsed laser beams at 1.06 μm we studied and optimized the performances of a ring self-pumped phase-conjugate mirror (Fig. 1). It has a lower threshold[13] than the commonly used total internal reflection phase-conjugate mirror. Moreover, it permits the insertion in the loop of optical elements to control the quality of the conjugate beam. Furthermore, it works even with a source of short coherence length,[14] which is essential for dynamic wave-front correction of pulsed lasers.

A. Steady-State Reflectivity

One important difference in the photorefractive effect between the cw and the nanosecond sources is their coherence length. Indeed, with a source of long coherence length compared with the loop length (cw illumination regime), both transmission and reflection gratings are recorded in the material. In the case of a short coherence length ($\sim$1.5 cm for our nanosecond source), only transmission gratings build up. In the cw illumination regime we used a piezo mirror vibrating at 20 Hz (Fig. 1) to wash out the reflection gratings.[14] We then verified that the energy requirements and the gratings involved are the same in both cw and nanosecond illumination regimes.[11] It is therefore reasonable to optimize the rise time and the reflectivity of the phase-conjugate mirror in the cw illumination regime, which provides easier experimental conditions.

As described in Ref. 13, the steady-state reflectivity of the ring phase-conjugate mirror depends on $\Gamma\ell$, where ℓ is the interaction length. As soon as $\Gamma\ell$ gets high enough, it saturates at a value equal to the transmission T of the loop. To confirm that the reflectivity had reached its maximum, we measured its steady-state value as a function of T for a grating spacing of $\Lambda = 1.6$ μm (Fig. 2). The reflectivity saturates for $T \geqslant 3\%$ (the curve is linear). Moreover, reflectivities as high as 70%, lim-

Table 1. Relevant Parameters for $BaTiO_3$:Rh Crystals Characterized at 1.06 μm in the cw Illumination Regime[a]

Measured Characteristics	Crystal			
	X16	X16-45	X17 6/3	X17 6/4
α	(0.07 ± 0.02) cm^{-1}	(0.12 ± 0.02) cm^{-1}	(0.06 ± 0.02) cm^{-1}	(0.05 ± 0.02) cm^{-1}
$\Delta\alpha$ (1.1 W cm^{-2})	(3.9 ± 0.2) m^{-1}	(5.7 ± 0.2) m^{-1}	(2.8 ± 0.2) m^{-1}	(3.6 ± 0.2) m^{-1}
$\left(\frac{\partial\Delta\alpha}{\partial t}\right)_{t=0,\ I=1.1\text{ W cm}^{-2}}$	(14 ± 4) m^{-1} s^{-1}	(11 ± 3) m^{-1} s^{-1}	(11 ± 3) m^{-1} s^{-1}	(13 ± 4) m^{-1} s^{-1}
τ_{ph} at 6.7 W cm^{-2}	(8 ± 1) s	(2 ± 0.5) s, $\beta = 45°$	(11 ± 1) s	(8 ± 1) s
$\tau_{\text{dark}}/\tau_{\text{ph}}$	240 ± 50	200 ± 40	90 ± 15	390 ± 70
Γ	2.05 cm^{-1}	0.6 cm^{-1}, $\beta = 45°$	2.6 cm^{-1}	2.5 cm^{-1}

[a] Crystals X16 and X17 are from two boules grown in similar conditions. Their characteristics are similar and prove that reasonably reproducible crystals can be grown. Measurements were performed with ordinary polarizations and $\beta = 0°$. Although they are given as examples, the values of τ_{ph} and Γ for X16-45 had to be measured with $\beta = 45°$ and cannot be directly compared with those obtained for the other samples.

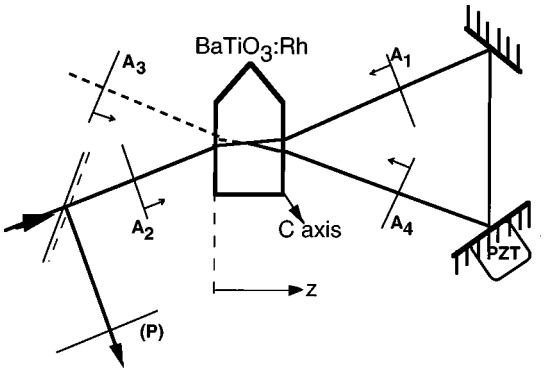

Fig. 1. Schematic of the ring self-pumped phase-conjugate mirror. Phase-conjugate beams are observed in optical plane (P). PZT, piezo mirror used in the cw illumination regime.

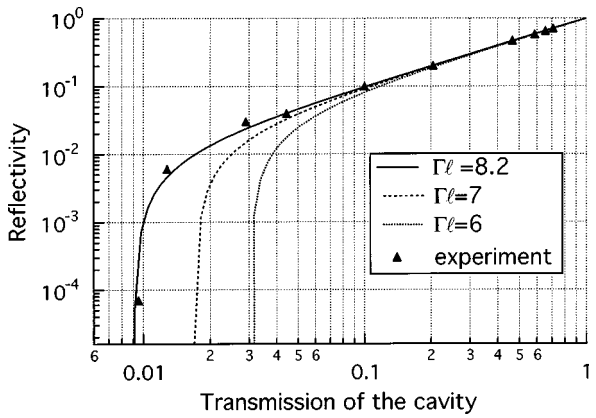

Fig. 2. Reflectivity of the ring self-pumped phase-conjugate mirror versus transmission of the loop in the cw illumination regime at 1.06 μm. Experimental data are fitted by theoretical curves obtained with different values of the product $\Gamma\ell$.

ited by T (71%), could be measured, so the photorefractive efficiency was found to be better than 90%. Figure 2 also shows that the sharp threshold of this phase-conjugate mirror corresponds to 1% of transmission. For a comparison with theory we computed, from the model developed in Ref. 13, the evolution of the steady-state reflectivity as a function of T for a given value of $\Gamma\ell$. The best fit to our measurements was obtained with $\Gamma\ell = 8.2$, in good agreement with the two-wave mixing measurements performed on another $BaTiO_3$: Rh crystal (referred to as Y32-B) in the cw illumination regime ($\Gamma = 23\ \mathrm{cm}^{-1}$) for $\ell = 3.5$ mm.[7]

B. Temporal Analysis

The time evolution of the reflectivity shows three distinct regions (Fig. 3). For $t \leqslant \tau_{10\%}$ (where $\tau_{10\%}$ is the time necessary for the reflectivity to reach 10% of its maximum), the phase-conjugate signal barely emerges from noise. For $\tau_{10\%} \leqslant t \leqslant \tau_{90\%}$, the reflectivity increases sharply. In the third region ($t > \tau_{90\%}$) the reflectivity saturates at its maximum value.

To optimize the rise time, we used a one-dimensional plane-wave model (Fig. 1),[13] assuming negligible absorption, an assumption that is valid for $BaTiO_3$: Rh at 1.06 μm ($\alpha = 0.1\ \mathrm{cm}^{-1}$). It cannot account for the spatial profile of the phase-conjugate beam, which can be described only by a three-dimensional model.[15] Furthermore, it does not take into account the influence of beam fanning, which was considered in Ref. 16. It also ignores the competition between the gratings generated by scattering at the very beginning of the process. However, as soon as the phase-conjugate reflectivity reaches 10% of its maximum one may consider that the parasitic gratings are negligible compared with the desired transmission grating. As we wish to optimize the reflectivity rise time $\tau_{90\%} - \tau_{10\%}$, this model is sufficient to permit us to describe roughly the four-wave mixing process.

With the notation of Fig. 1, the coupled-wave equations for the transmission grating without absorption are

$$\frac{\partial A_1(z,t)}{\partial z} = i\frac{\Gamma}{4E_{sc}}E_1(z,t)A_4(z,t),$$

$$\frac{\partial A_2{}^*(z,t)}{\partial z} = i\frac{\Gamma}{4E_{sc}}E_1(z,t)A_3{}^*(z,t),$$

$$\frac{\partial A_3(z,t)}{\partial z} = -i\frac{\Gamma}{4E_{sc}}E_1(z,t)A_2(z,t),$$

$$\frac{\partial A_4{}^*(z,t)}{\partial z} = -i\frac{\Gamma}{4E_{sc}}E_1(z,t)A_1{}^*(z,t), \qquad (1)$$

where A_1–A_4 are the complex amplitudes of the plane waves and E_{sc} is the steady-state space-charge field.

It is now proved that the three charge states of rhodium (Rh^{3+}, Rh^{4+}, Rh^{5+}) are responsible for the photorefractive effect in $BaTiO_3$:Rh (Ref. 17) and that a three-charge state model is suitable.[12,18] However, we used for simplification the classic single-carrier single-site model without an applied electric field to describe the time evolution of the space-charge field, which gives the well-known equation[19]

$$\frac{\partial E_1(z,t)}{\partial t} = -\frac{1}{\tau_{ph}}[E_1(z,t) - im(z,t)E_{sc}], \qquad (2)$$

where τ_{ph} is the photorefractive time constant for a given grating spacing and, for a given $I_0 = \Sigma_i|A_i|^2$, $m(z,t)$, is the modulation of the interference pattern defined by

$$m(z,t) = 2(A_1A_4{}^* + A_2{}^*A_3)/I_0. \qquad (3)$$

We assume that the initial seeding amplitude A_3 results from a scattering at the input surface: $A_3(z, t = 0)$

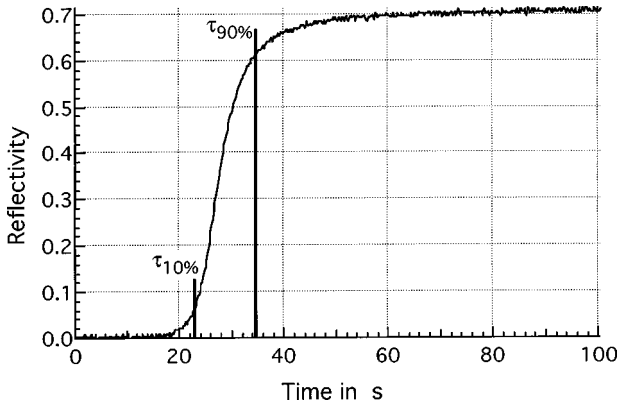

Fig. 3. Typical experimental time evolution of the reflectivity of the ring self-pumped phase-conjugate mirror at 1.06 μm in the cw illumination regime. This curve is obtained for an intensity of 5 W cm^{-2}.

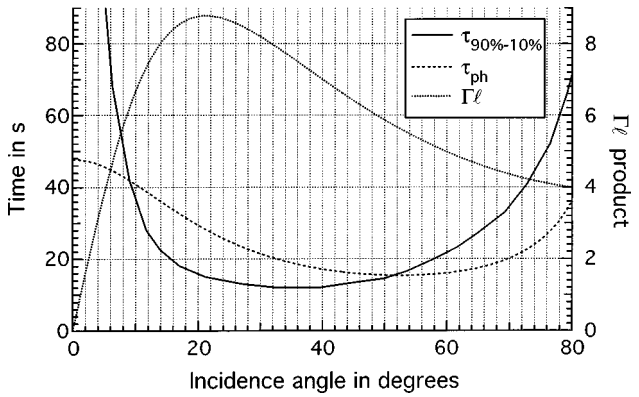

Fig. 4. Predicted $\Gamma\ell$, photorefractive rise time τ_{ph}, and reflectivity rise time $\tau_{90\%} - \tau_{10\%}$ versus incidence angle θ on the photorefractive crystal (see text for choice of parameters).

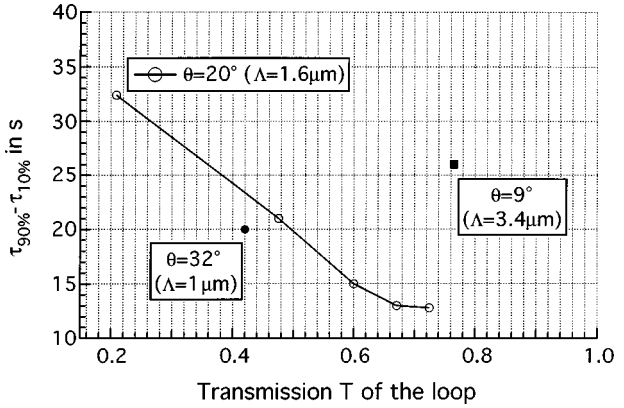

Fig. 5. Experimental values of $\tau_{90\%} - \tau_{10\%}$ for several incidence angles θ. To compensate for the variations of transmission T of the loop with θ, for a given θ $\tau_{90\%} - \tau_{10\%}$ is to be compared with the value obtained at $\theta = 20°$ for the same T.

$= \epsilon$. This initial condition has no consequence for $\tau_{90\%} - \tau_{10\%}$ as soon as ϵ is small enough. For a given I_0 the important features for the kinetics of the phase conjugation are τ_{ph}, $\Gamma\ell$, and transmission T, as in photorefractive oscillators.[20] We can obtain $\tau_{90\%} - \tau_{10\%}$, for a given incidence θ, by inserting the values of τ_{ph} and $\Gamma\ell$ into the coupled-wave equations and solving them numerically. The result is plotted in Fig. 4 for $T = 100\%$, an incident beam intensity of 5 W cm^{-2}, and a 45° cut crystal of thickness 3.5 mm with a typical $N_{eff} \approx 5 \times 10^{16}$ cm^{-3}. The relevant electro-optic coefficients are those given in Ref. 21. The reflectivity rise time appears to be minimized for an incidence θ between 20° and 50° ($0.7\ \mu m \leqslant \Lambda \leqslant 1.6\ \mu m$). The increase in the rise time for $\theta \leqslant 20°$ is caused by the decay of $\Gamma\ell$, whereas that at $\theta \geqslant 50°$ results from the decay of illumination inside the sample because of refraction. We verified this result experimentally for three values of θ. But, as T changes with θ, we compared the reflectivity rise time for $\theta = 9°$ and $\theta = 32°$ with the value obtained at $\theta = 20°$ for the same transmission T, as shown in Fig. 5. At $\theta = 32°$ and $T \approx 42\%$, $\tau_{90\%} - \tau_{10\%} = 20$ s is slightly smaller than the value obtained with the same T at $\theta = 20°$. At $\theta = 9°$ and $T \approx 76\%$, $\tau_{90\%} - \tau_{10\%} = 26$ s is much higher than the rise time at $\theta = 20°$ for the same value of T. In agreement with our simplified model, the reflectivity rise time seldom varies between $\theta = 20°$ and $\theta = 32°$ (Fig. 4), whereas small angles ensure a better overlap, in the volume of the crystal, of beams of limited cross section. For the chosen incidence angle of 20° ($\Lambda = 1.6\ \mu m$) and for $T = 71\%$ we measured a reflectivity of 70% and $\tau_{90\%} - \tau_{10\%} = 12$ s for an incident intensity of 5 W cm^{-2}, corresponding to an energy of $E_{10\% \to 90\%} = 60$ J cm^{-2}.

4. PHASE CONJUGATION IN THE NANOSECOND ILLUMINATION REGIME

We used a Q-switched Nd:YAG laser, intracavity filtered to provide a TEM_{00} mode, which delivers 5-mJ, 10-ns pulses at 1.06 μm at a repetition rate of 10 Hz. In the ring self-pumped phase-conjugate mirror a three-prism system achieves a rotation of 90° of the beam cross section and realizes a good selection of the phase-conjugate beam (Fig. 6).[22] Two half-wave plates preserve the extraordinary polarization on the crystal that is required for high photorefractive gains. This system was successfully used at 532 nm.[23] Unlike lenses that could also select the conjugate beam,[22] it avoids focusing of the beams and is therefore more suitable for use with high-power pulses. It improves the phase-conjugation fidelity, as illustrated in Fig. 7. The three images are observed in the same optical plane. The vertical structure in the phase-conjugate beam profile for a loop built with the usual mirrors disappears with the three-prism system. With the three-prism system we measured $E_{10\% \to 90\%} = 90$ J cm^{-2} for a transmission of the loop of 79%, which is only slightly more than the fluence required in the cw illumination regime. The reflectivity was also saturated at its maximum value of 79%. The difference in the required fluence for nanosecond and cw illuminations can be attributed to the change in the measured two-beam coupling gain between the two illumination regimes, as shown in Ref. 8 for another $BaTiO_3$:Rh crystal. A weak decrease of the product $\Gamma\ell$ leads to an increase of the time constant of the four-wave mixing process.

5. RESPONSE TO AN ABRUPT CHANGE IN THE WAVE FRONT IN THE INCIDENT BEAM

Efficient phase conjugation can be performed by other nonlinear media. Stimulated Brillouin scattering is com-

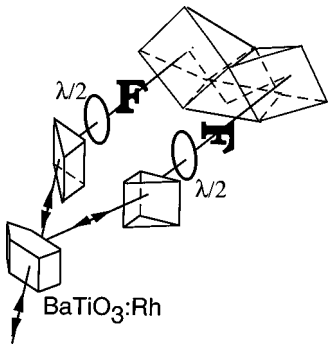

Fig. 6. Ring self-pumped phase-conjugate mirror with a three-prism system performing a 90° rotation of the beam cross section. The loop length is 12 cm.

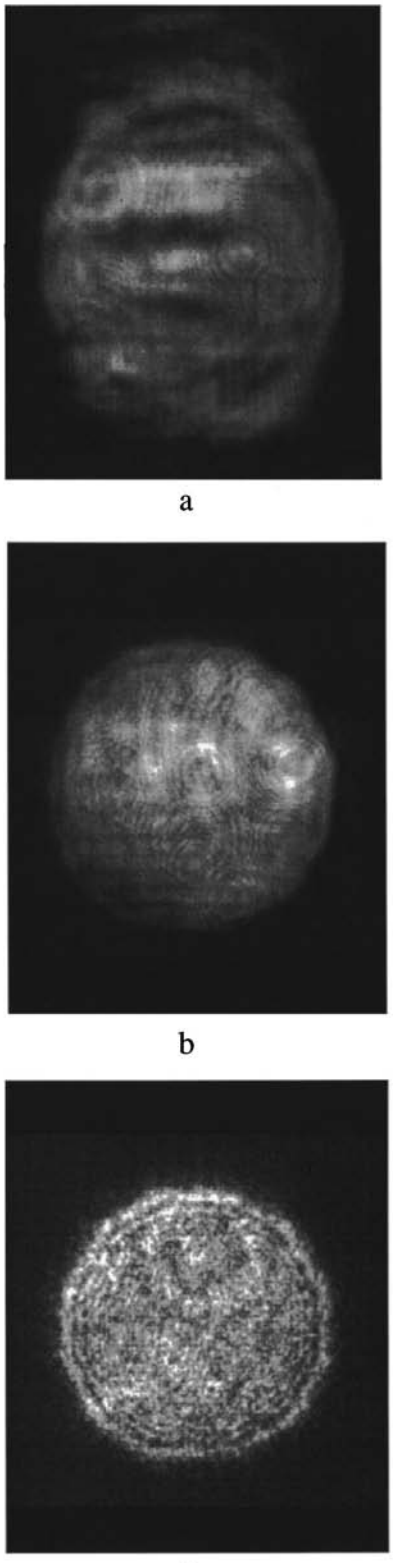

Fig. 7. a, Phase-conjugate beam profile from a loop using conventional mirrors. The poor fidelity of the phase conjugation appears in the vertical structure of the image. b, Phase-conjugate beam profile with the three prisms. c, Incident beam profile. All the images were obtained in the nanosecond illumination regime at 1.06 μm.

mercially used in a Nd:YAG laser source for pulse-to-pulse phase conjugation.[24] In photorefractive $BaTiO_3$:Rh crystals the effect is sensitive to the accumulation of energy. As a consequence, an abrupt change in the wave front of the incident beam decreases the reflectivity, as described in Ref. 25. What does the phase-conjugate beam look like? This problem is of interest for the dynamic wave-front correction of nanosecond laser sources. Indeed, such wave-front-corrected lasers should be efficient for different repetition rates. When the operator changes this rate (for instance, from 10 to 100 Hz), the thermal lens induced in the Nd:YAG amplifier rod changes its focal length.

We modeled the effect as follows: Steady-state phase conjugation is reached for a given incident reference wavefront (subscript R). We assume that the incident beam is a spherical wave created by a thermal lens of focal length much longer than the length of the phase-conjugate mirror loop. At steady state, the two pump beams (beams 3 and 4) are phase conjugates of each other (Fig. 1). Therefore, at steady state, if A_{2R} converges at C_{2R} $(x_{2R}, 0, z_{2R})$, A_{3R}, which is the phase conjugate of wave 4, diverges from C_{3R} $(x_{3R}, 0, z_{3R})$, which is the image of C_{2R} by the loop (Fig. 8). Its coordinates become $(x_{2R}, 0, -z_{2R})$ if the loop length is neglected. With the notation of Fig. 8, for a symmetrical incidence upon the crystal and in the paraxial approximation the steady-state transmission grating (the only one existing here) results from the interference of the two waves:

$$\mathbf{A}_{2R} = \hat{e}_y \frac{a_{2R}}{r_{2R}} \exp(-i\omega t)\exp[ik(z - z_{2R})] \times \exp\left\{\frac{-i\pi}{\lambda z_{2R}}[(x - x_{2R})^2 + y^2]\left(1 + \frac{z}{z_{2R}}\right)\right\}, \tag{4}$$

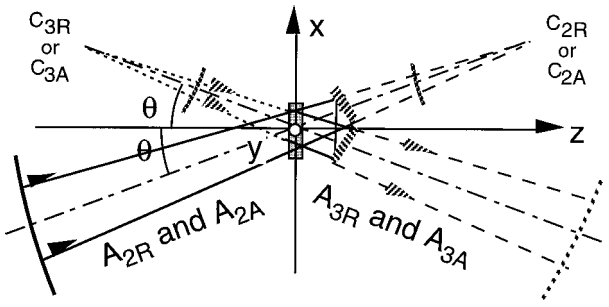

Fig. 8. Notation used in Section 5. $y = 0$ is the incidence plane. The mirror signs represent the loop mirrors. The loop length is assumed to be much smaller than the focal length of the thermal lens to be corrected for. Wave A_{2R} converges at C_{2R} $(x_{2R}, 0, z_{2R})$. At steady state it is diffracted as A_{3R} originating from C_{3R} $(x_{2R}, 0, -z_{2R})$. The photorefractive crystal is centered at (0, 0, 0). A_{2A} is the wave resulting from an abrupt change in the thermal lens; it is now converging at C_{2A} $(x_{2A}, 0, z_{2A})$; it is diffracted as A_{3A} originating from C_{3A} $(x_{3A}, 0, -z_{3A})$.

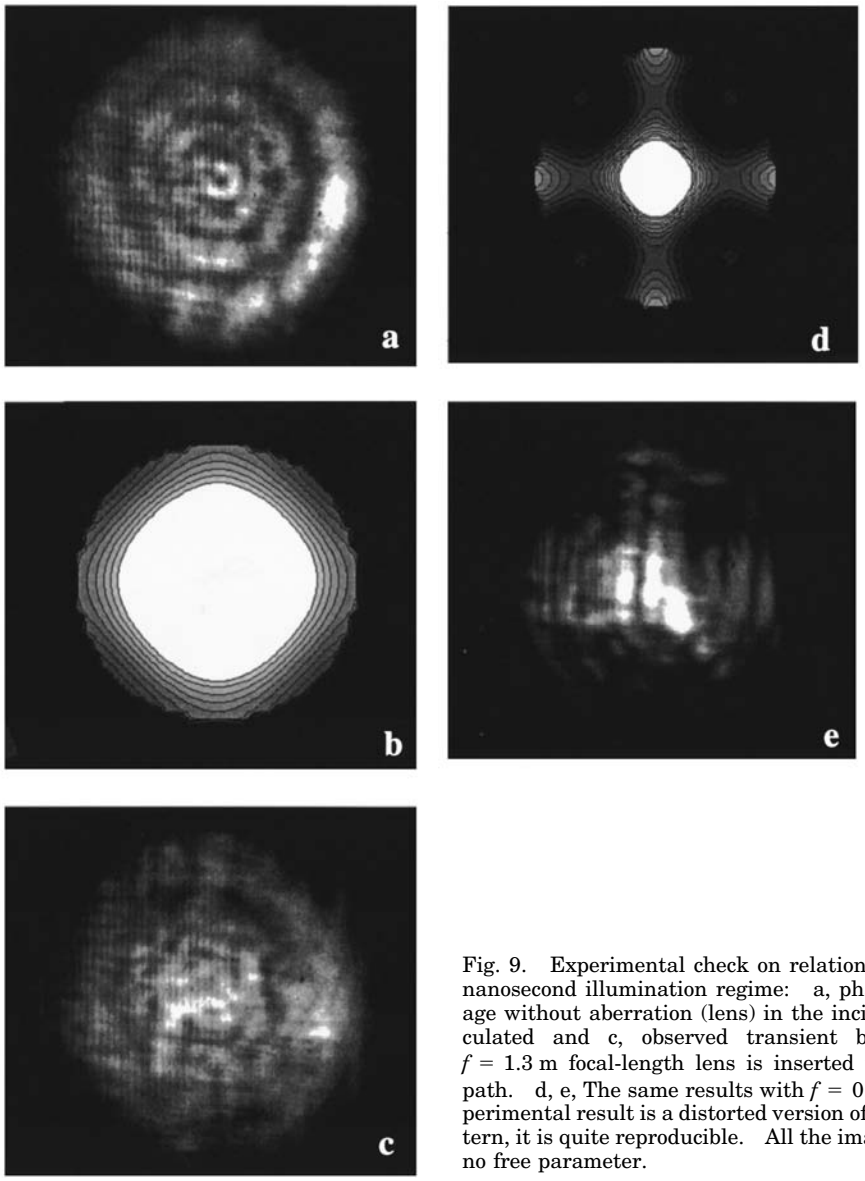

Fig. 9. Experimental check on relation (13) at 1.06 μm in the nanosecond illumination regime: a, phase-conjugate beam image without aberration (lens) in the incident beam path; b, calculated and c, observed transient beam image when an $f = 1.3$ m focal-length lens is inserted into the incident beam path. d, e, The same results with $f = 0.5$ m. Although the experimental result is a distorted version of the predicted cross pattern, it is quite reproducible. All the images are calculated with no free parameter.

$$\mathbf{A}_{3R} = \hat{e}_y \frac{a_{3R}}{r_{2R}} \exp(-i\omega t)\exp[ik(z + z_{2R})] \times \exp\left\{\frac{i\pi}{\lambda z_{2R}}[(x - x_{2R})^2 + y^2]\left(1 - \frac{z}{z_{2R}}\right)\right\}, \tag{5}$$

where $\hat{e}_y$ is a unit vector along the y axis. $\mathbf{A}_{2R}$ is a converging wave; $\mathbf{A}_{3R}$ is a diverging wave. Their respective amplitudes a_{2R}/r_{2R} and a_{3R}/r_{2R} are assumed to be constant on the thickness of the photorefractive crystal. $k = 2\pi/\lambda$ is the wave number.

The induced photorefractive index modulation has the following spatial variations:

$$\Delta n \propto \Delta n_0 \exp(2ikz_{2R})\exp\left\{2i\frac{\pi}{\lambda z_{2R}}[(x - x_{2R})^2 + y^2]\right\}. \tag{6}$$

We consider an abrupt change in the curvature of the incident spherical wave; the focal length of the thermal lens changes abruptly. For this aberrated wave we use the subscript A:

$$\mathbf{A}_{2A} = \hat{e}_y \frac{a_{2A}}{r_{2A}} \exp(-i\omega t)\exp[ik(z - z_{2A})] \times \exp\left\{\frac{-i\pi}{\lambda z_{2A}}[(x - x_{2A})^2 + y^2]\left(1 + \frac{z}{z_{2A}}\right)\right\}, \tag{7}$$

with an amplitude a_{2A}/r_{2A} constant on the thickness of the material. Although such is probably not the case for a ring self-pumped phase-conjugate mirror starting from noise, we assume here for simplification that wave 2 is not depleted. Then the equation of propagation is

$$\nabla^2\mathbf{A}_{3A} + k^2\mathbf{A}_{3A} = -k^2\frac{[\Delta\varepsilon]}{n^2}\mathbf{A}_{2A}, \tag{8}$$

where $[\Delta\varepsilon]$ is a perturbation of the relative dielectric tensor at optical frequencies and n is the refractive index:

$$\hat{e}_y^* \cdot [\Delta\varepsilon] \cdot \hat{e}_y = 2n\Delta n. \tag{9}$$

The solution is the sum of spherical waves of the form

$$\mathbf{A}_{3A} = \hat{e}_y \frac{a_{3A}(x, y, z)}{r_{3A}} \exp(-i\omega t)\exp[ik(z + z_{3A})] \times \exp\left\{\frac{i\pi}{\lambda z_{3A}}[(x - x_{3A})^2 + y^2]\left(1 - \frac{z}{z_{3A}}\right)\right\}, \tag{10}$$

where $a_{3A}(x, y, z)$ do not include spatially varying phase terms. Substituting Eq. (10) into Eq. (8), we obtain a single diffracted spherical wave that fulfills the relations

$$\frac{x_{3A}}{z_{3A}} = \frac{x_{2A}}{z_{2A}} = \frac{x_{2R}}{z_{2R}}, \qquad \frac{1}{z_{3A}} + \frac{1}{z_{2A}} = \frac{2}{z_{2R}}, \tag{11}$$

where we find that

$$a_{3A}(\ell) \propto \operatorname{sinc}\left\{\left[\frac{(x - x_{3A})^2 + y^2}{{z_{3A}}^2} - \frac{(x - x_{2A})^2 + y^2}{{z_{2A}}^2}\right]\frac{\ell}{2\lambda}\right\}. \tag{12}$$

Relations (11) account for the fact that waves $\mathbf{A}_{2A}$ and $\mathbf{A}_{2R}$ propagate in the same direction and that the grating behaves as a lens in the paraxial approximation. The term $\operatorname{sinc}(u) = \sin(\pi u)/\pi u$ in relation (12) reflects the Bragg selectivity of the thick hologram. In a more accurate model that takes into account pump depletion, the strength of the grating would appear in the Bragg selectivity term. Here, this term depends on the spatial variables x and y.

Output wave $\mathbf{A}_{1A}$ is the coherent superposition of the diffracted wave from $\mathbf{A}_{4A}$ and of the transmitted wave of $\mathbf{A}_{3A}$ after its 90° cross-section rotation through the three-prism system. Then the output intensity is proportional to a Bragg selectivity term of the form

$$I \propto \left|\operatorname{sinc}\left\{\left[\frac{(x - x_{3A})^2 + y^2}{{z_{3A}}^2} - \frac{(x - x_{2A})^2 + y^2}{{z_{2A}}^2}\right]\frac{\ell}{2\lambda}\right\} + \operatorname{sinc}\left\{\left[\frac{(y - x_{3A})^2 + x^2}{{z_{3A}}^2} - \frac{(y - x_{2A})^2 + x^2}{{z_{2A}}^2}\right]\frac{\ell}{2\lambda}\right\}\right|^2. \tag{13}$$

We experimentally verified this result by using a nearly collimated beam as an incident beam (Fig. 9) at 1.06 μm in the nanosecond illumination regime in the ring phase-conjugate mirror described in Section 4. The incidence angle of waves $\mathbf{A}_{2R}$ and $\mathbf{A}_{2A}$ was 20°. We obtained aberrated wave $\mathbf{A}_{2A}$ by inserting into the incident beam lenses of various focal lengths much longer than the loop length (12 cm). The beam diameter before the additional lens was limited to 3 mm by a diaphragm. We obtained the images by collecting the phase-conjugate beam with a beam splitter, as in Fig. 1, and by imaging the $BaTiO_3$:Rh crystal onto a CCD camera. The rings on reference

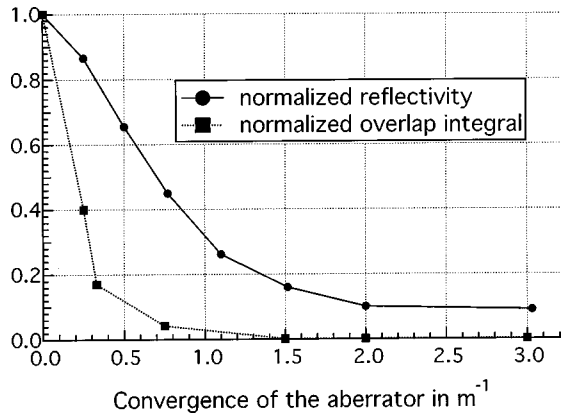

Fig. 10. Computed variations of the reflectivity and of the overlap integral between the real and the expected transient phase-conjugate beams versus the convergence of the aberrator introduced on the incident collimated beam. For clarity these values are normalized to their maxima.

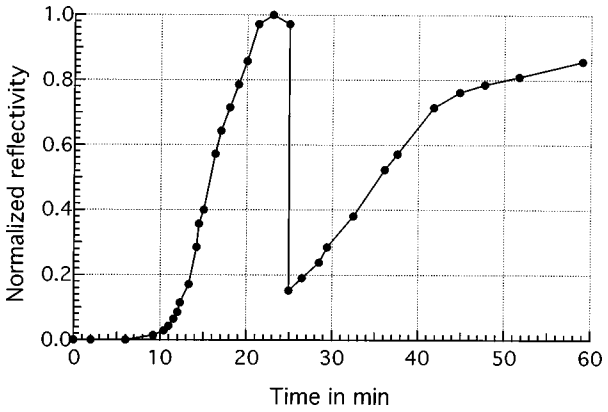

Fig. 11. Experimental time evolution of the reflectivity. At t = 25 min a diverging lens ($f = -1$ m) is introduced into the incident beam. The slower recovery is caused by the poor overlap integral between the transient diffracted beam and the phase-conjugate beam obtained only at steady state.

steady-state phase-conjugate beam A_{1R} (Fig. 9a) are caused by diffraction from the diaphragm. The transient phase-conjugate images (Figs. 9b and 9d) predicted (with no free parameter) by relation (13) are in qualitative agreement with the observed ones (Figs. 9c and 9e). As calculated numerically from relation (13), in the case of a nearly collimated incident wave the reflectivity falls (Fig. 10) with the convergence of the added aberrator. Even sharper is the drop in phase-conjugate fidelity, estimated numerically by the overlap integral between the steady-state and the transient phase-conjugate waves (Fig. 10). For instance, with a given aberrator, if the reflectivity falls to 20%, the overlap integral drops to 1%. Therefore the grating corresponding to the steady-state phase-conjugate wave has to build up from nearly zero while the previously recorded one decays. The time needed to rebuild the steady-state reflectivity is much longer than the $\tau_{90\%} - \tau_{20\%}$ that could be expected from the 20% reflectivity. Actually, it is quite close to the time needed if no grating had previously been recorded in the crystal. This fact is important for applications and is illustrated in Fig. 11. This experiment was performed in the nanosecond illumination regime with the three-prism system; $\tau_{90\%}$

$-$ $\tau_{10\%} \approx 7$ min and $\tau_{90\%} \approx 21$ min for the first buildup. At $t = 25$ min a diverging lens ($f = -1$ m) is inserted into the incident beam. The reflectivity drops to 15%, and the time necessary to recover the steady state is ~25 min, i.e., much larger than the $\tau_{90\%} - \tau_{15\%} \approx 6$ min estimated from the first rise.

We also verified that the beam profile corresponds to a phase-conjugate profile (Fig. 9a) only at steady state. Relevant characteristics to be measured in such a dynamic phase-conjugate mirror would be the kinetics of the phase-conjugate fidelity and the value of the reflectivity at steady state.

6. CONCLUSIONS

We have shown that reproducible crystals of $BaTiO_3$:Rh can be grown that prove to be well suited for applications at 1.06 μm. We used these crystals to optimize a ring self-pumped phase-conjugate mirror. In the cw illumination regime the mirror exhibited 70% reflectivity for 71% transmission of the loop, and a density of energy of 60 J cm^{-2} was needed to increase the reflectivity from 10% to 90% of its maximum value. In the nanosecond illumination regime this figure increases to 90 J cm^{-2}, and reflectivities equal to the transmission of the loop (79%) have been measured. We have shown that the fidelity of the phase conjugation is strongly affected by an abrupt change of the incident wave front and is restored when the reflectivity gets back to its steady-state value. These properties, along with the possibility of inserting optical elements to select the phase-conjugate beam in such a ring self-pumped phase-conjugate mirror, are attractive for dynamic wave-front correction of nanosecond Nd: YAG lasers, as is done with the internal loop geometry.[25]

ACKNOWLEDGMENT

We thank Gilles Pauliat for continuous support and productive discussions.

REFERENCES

1. L. Mager, G. Pauliat, D. Rytz, and G. Roosen, in *Novel Optical Materials & Applications*, I. C. Khoo, F. Simoni, and C. Umeton, eds. (Wiley, New York, 1996), Chap. 6, pp. 149–174.
2. S. MacCormack, G. D. Bacher, J. Feinberg, S. O'Brien, R. J. Lang, M. B. Klein, and B. A. Wechsler, "Powerful, diffraction limited semiconductor laser using photorefractive beam coupling," Opt. Lett. **22**, 227 (1997).
3. J. M. Verdiell, H. Rajbenbach, and J. P. Huignard, "Injection-locking of gain-guided diode laser arrays: influence of the master beam shape," IEEE Photonics Technol. Lett. **2**, 568 (1990).
4. M. Cronin-Golomb, K. Y. Lau, and A. Yariv, "Infrared photorefractive passive phase conjugation with $BaTiO_3$: demonstration with GaAlAs and 1.09 μm Ar^+ lasers," Appl. Phys. Lett. **47**, 567 (1985).
5. B. A. Wechsler, M. B. Klein, C. C. Nelson, and R. N. Schwartz, "Spectroscopic and photorefractive properties of infrared-sensitive rhodium-doped barium titanate," Opt. Lett. **19**, 536 (1994).
6. A. Brignon, D. Geffroy, J. P. Huignard, M. H. Garrett, and I. Mnushkina, "Experimental investigations of the photorefractive properties of rhodium-doped $BaTiO_3$ at 1.06 μm," Opt. Commun. **137**, 311 (1997).
7. N. Huot, J. M. C. Jonathan, G. Pauliat, D. Rytz, and G. Roosen, "Characterization of a photorefractive rhodium doped barium titanate at 1.06 μm," Opt. Commun. **135**, 133 (1997).
8. N. Huot, J. M. C. Jonathan, G. Roosen, and D. Rytz, "Two-wave mixing in photorefractive $BaTiO_3$:Rh at 1.06 μm in the nanosecond regime," Opt. Lett. **22**, 976 (1997).
9. G. C. Valley, "Short pulse grating formation in photorefractive materials," IEEE J. Quantum Electron. **QE-19**, 1637 (1983).
10. M. J. Damzen and N. Barry, "Intensity-dependent hole–electron competition and photocarrier saturation in $BaTiO_3$ when using intense laser pulses," J. Opt. Soc. Am. B **10**, 600 (1993).
11. N. Huot, J. M. C. Jonathan, G. Roosen, and D. Rytz, "Self-pumped phase conjugation in a ring cavity at 1.06 μm in the cw and nanosecond regimes using photorefractive $BaTiO_3$:Rh," Opt. Commun. **140**, 296 (1997).
12. N. Huot, J. M. C. Jonathan, and G. Roosen, "Validity of the three charge state model in photorefractive $BaTiO_3$:Rh at 1.06 μm in the cw regime," Appl. Phys. B **65**, 489 (1997).
13. M. Cronin-Golomb, B. Fischer, J. O. White, and A. Yariv, "Theory and applications of four wave mixing in photorefractive media," IEEE J. Quantum Electron. **QE-20**, 12 (1984).
14. M. Cronin-Golomb, J. Paslaski, and A. Yariv, "Vibration resistance, short coherence length operation, and mode-locked pumping in passive phase conjugate mirrors," Appl. Phys. Lett. **47**, 1131 (1985).
15. V. T. Tikhonchuk and A. A. Zozulya, "Structure of light beams in self-pumped four-wave mixing geometries for phase conjugation and mutual conjugation," Prog. Quantum Electron. **15**, 231 (1991).
16. N. V. Bogodaev, L. I. Ivleva, A. S. Korshunov, A. V. Mamaev, N. N. Poloskov, and A. A. Zozulya, "Geometry of a self-pumped passive ring mirror in crystals with strong fanning," J. Opt. Soc. Am. B **10**, 1054 (1993).
17. H. Kröse, R. Scharfschwerdt, O. F. Schirmer, and H. Hesse, "Light-induced charge transport in $BaTiO_3$ via three charge states of rhodium," Appl. Phys. B: Photophys. Laser Chem. **61**, 1 (1995).
18. K. Buse, "Light-induced charge transport processes in photorefractive crystals. I. Models and experimental methods," Appl. Phys. B **64**, 273 (1997).
19. N. V. Kukhtarev, V. B. Markov, S. G. Odulov, M. S. Soskin, and V. L. Vinetskii, "Holographic storage in electrooptic crystals," Ferroelectrics **22**, 949 (1979).
20. G. Pauliat, M. Ingold, and P. Günter, "Analysis of the build up of oscillations in self-induced photorefractive light resonators," IEEE J. Quantum Electron. **25**, 201 (1989).
21. P. Bernasconi, M. Zgonik, and P. Günter, "Temperature dependence and dispersion of electro-optic and elasto-optic effect in perovskite crystals," J. Appl. Phys. **78**, 2651 (1995).
22. S. A. Korolkov, Y. S. Kuzminov, A. V. Mamaev, V. V. Skhunov, and A. A. Zozulya, "Spatial structure of scattered radiation in a self-pumped photorefractive passive ring mirror," J. Opt. Soc. Am. B **9**, 664 (1992).
23. L. Mager, C. Lacquarnoy, G. Pauliat, M. H. Garrett, D. Rytz, and G. Roosen, "High-quality self-pumped phase conjugation of nanosecond pulses at 532 nm using photorefractive $BaTiO_3$," Opt. Lett. **19**, 1508 (1994).
24. J. K. Timinski, C. D. Nabors, G. Frangineas, and D. K. Negus, in *Advanced Solid-State Lasers*, Vol. 24 of OSA Proceedings Series (Optical Society of America, Washington, D.C., 1995), paper MD2.
25. A. Brignon, J. P. Huignard, M. H. Garrett, and I. Mnushkina, "Nd:YAG master-oscillator power amplifier with a rhodium-doped $BaTiO_3$ self-pumped phase-conjugate mirror," Opt. Lett. **22**, 442 (1997).